https://doi.org/10.17221/772/2017-PSE

Variability of tomato in protected environment in response to meteorological parameters

Francesca SANNA[1,3,*], Roberto DEBOLI[2], Angela CALVO[1]

[1]*Department of Agriculture, Forest and Food Sciences (DiSAFA), University of Turin, Turin, Italy*
[2]*Institute for Agricultural and Earthmoving Machines – National Research Council (IMAMOTER-CNR), Turin, Italy*
[3]*National Institute of Metrological Research (INRiM), Turin, Italy*
**Corresponding author: francesca.sanna@unito.it*

ABSTRACT

Sanna F., Deboli R., Calvo A. (2018): Variability of tomato in protected environment in response to meteorological parameters. Plant Soil Environ., 64: 247–254.

An experimental site for the measurement of meteorological parameters in protected environment and the evaluation of the tomato cultivar variability is presented in this paper. The site was equipped with cultivation structures with different covering materials and calibrated sensors traceable to the International System of Units. The microclimate conditions were monitored by sensors for solar radiation (from 290 nm to 2800 nm), air temperature (from –10°C to 40°C) and relative humidity (from 10% RH to 98% RH) inside and outside the tunnels. Specific procedures were used to calibrate the instruments. The following aspects were evaluated: microclimate and solar radiation within different cultivations; morphological observations of the tomatoes in response to the different environments; optical and radiometric properties of the films used as covering material. High temperatures recorded (over 40°C) changed the transmissive feature of the films and consequently affected the growth, anthesis, leaf area index and fruit setting of tomatoes.

Keywords: metrology; *Lycopersicon esculentum* Mill.; calibration uncertainty; meteorological measurements

Solar radiation (SR) is an important parameter for plants because it provides the energy for photosynthesis and modulates growth and development in response to environmental conditions. Plants have the ability to monitor intensity, spectral distribution, direction and daily duration of the direct and incident light (Li and Yang 2015).

When operating in protected cultivation, the amount and the spectral distribution of SR inside the cultivation environment undergo modifications that depend on the type of the cover used. The productivity of a protected crop is highly correlated to the amount of electromagnetic radiation received, which in turn depends on the amount of ultraviolet (UV), visible (photosynthetically active radiation (PAR)), and infrared (IR) radiation transmitted through the cover material of these structures (Krizek 2004).

Studies aimed at quantifying the effects of UV on crop quality led to unclear results. Indeed, data take into account some aspects of the problem separately, such as physiological, production or quality (Bacci et al. 1999, Castagna et al. 2013). Particularly, the increase in UV-B (280–315 nm) is a potential risk to the physiology and the plants growth, as it can damage DNA, proteins, cell membranes, and affect the physiologic function (Fedina and Velitchkova 2009). However, subsequent research showed that comparatively low doses of SR in plants induce a metabolic response to stress

https://doi.org/10.17221/772/2017-PSE

plant resistance, which leads to an increase of molecules with high antioxidant capacity (Schreiner and Huyskens-Keil 2006).

Physiological parameters, such as seed dormancy, gases produced during the germination and in the period immediately after harvest are affected by meteorological parameters i.e. temperature (T), SR and precipitation that in turn, affect the variability of crop productivity (Fišerová et al. 2015).

On the other hand, instruments that measure SR need constant maintenance and calibration to obtain UV measurements of required quality (Hülsen and Gröbner 2007). The calibration values were underestimated or neglected for a long time. It was shown that the introduction of the measurement uncertainty for ground-based spectroradiometric measurements increases significantly the reliability of the measured data (Schaepman 1998).

Moreover, calibration of the weather sensors installed in agriculture sites is usually not performed or carried out for comparison before installation. Reference sensors are not always made to operate in open air, therefore, it is not possible to cover the whole range for the quantities and the mutual influences evaluation among parameters is not achievable (Sanna et al. 2018).

On the basis of the experience acquired in metrology for agro-meteorology (Sanna et al. 2014, Merlone et al. 2018), an experimental site equipped with cultivation structures (tunnel type) and calibrated sensors for the measurements of meteorological parameters was assembled. The research activities concerned the quality of table tomatoes (*Lycopersicon esculentum*, cv. Saint Pierre) grown in protected environment. The following aspects were evaluated:

– microclimate conditions: air T in the range (–10–40)°C, relative humidity (RH) range 10–98% RH with a target uncertainty of 0.3°C and 5% RH, respectively; UV-B in the spectral range 290–315 nm;
– crops growth in response to the type of plastic film adopted and the different microclimate environments;
– radiometric properties of the covering materials due to their exposure to the SR and deterioration.

This paper presents the results for the measurement of meteorological parameters in protected cultivation and the assessment of product variability of a tomato cultivar in an experimental site located in Northern Italy.

MATERIAL AND METHODS

Experimental site set up. The experimental measurement site was located at the Research Area of National Research Council, Turin. The following structure and instruments were installed: 2 adjacent tunnels (called IN-C and IN-B) of equal size with different covering material having opposite filtering properties with respect to UV-B SR. The first type was transmissive, the second diffusive and filtered the UV-B SR; 2 automatic weather stations (AWS, MTX Srl, Campogalliano, Modena, Italy), one per tunnel, including sensors for the detection of air T, RH and UV-B; 1 AWS outside the tunnels (OUT), including sensors for the detection of T, RH and UV-B.

Cultivar. On 20 May 2016, 46 seedlings of Saint Pierre tomato cultivar, previously sown in a microclimate-controlled greenhouse, were selected, transplanted in individual pots and moved in the site (20 per tunnel and 6 outside). A drip irrigation system was installed to control the amount of water and fertilizer supplied (Biswas et al. 2015).

During the tomatoes' growing period, several phenological aspects were recorded: plant growth, leaf area index (LAI), anthesis and fruit set. The plant growth was calculated by measuring the stem from the collar to the apical meristem. The result of each measurement of LAI by means of the app PocketLAI (Confalonieri et al. 2013) was in turn the result of the mean of three measurements performed on the same plant, one every 10 s. Anthesis is given here as appearance of a flower for each flowering, counted up to five (100 flowers for each tunnel and 30 outside). Fruit set means the onset of the first fruits for each flowering for a maximum of three fruits (300 fruits for each tunnel and 90 fruits outside).

Meteorological instruments. The meteorological instruments were calibrated by means of procedures defined *ad hoc*. The air T and RH sensors were calibrated using the 'EDIE – earth dynamics investigation experiment' device (Lopardo et al. 2015), developed under the European ENV07 MeteoMet project (Merlone et al. 2015) equipped with a Pt100 PRT (Platinum Resistance Thermometers, 5615-6-Fluke, Fluke Italia Srl, Brugherio, Italy), calibrated at the fixed points of the International Temperature Scale (ITS-90), used as a reference sensor.

In order to cover the whole range of atmospheric measurements, the selected set points were: –20°C,

https://doi.org/10.17221/772/2017-PSE

–10°C, 0°C, 10°C, 25°C, and 45°C for T sensors; 30%, 60%, 75% and 90% RH for RH sensors, plus a second point at 60% rh for the evaluation of the hysteresis. T data were recorded by a thermometry bridge (1594A – Fluke, Fluke Italia Srl, Brugherio, Italy) with a sampling recording time of 10 s. The repeatability was assumed with the standard deviation of the readings along 5 min. In the calculation of the expanded uncertainty (U) the sources of uncertainty for T and RH measurements as listed in Table 1 were taken into account. The interpolation uncertainty (U_{int}) was obtained by calculating the square root of the quadratic sum of the residuals, i.e. the differences between the measured values and those calculated with the interpolating polynomial, divided by degrees of freedom.

The values of the calibration uncertainty were 0.264°C; 0.259°C and 0.267°C for T and 2.559%; 3.169% and 3.159% for RH in sensors A/IN-C, B/IN-B, C/OUT, respectively (Table 1), meeting the target of calibration uncertainty proposed. The U is expressed as standard uncertainty multiplied by the coverage factor k = 2, which for a normal distribution corresponds to a confidence level of 95%. The standard measurement uncertainty associated to hysteresis was within 1%. UV-B SR and pyranometer sensors were calibrated with a reference pyranometer Ph. Schenk 8101, ISO 9060 (1990) First Class. In Table 2 the calibration results are listed. The meteorological parameters were acquired with an interval of 15 min, and hourly and daily averages were calculated.

Covering materials. The optical properties of the polymers are correlated to the structure of the polymer itself and its degree of crystallinity. The index of refraction n of a material is an optical feature, dimensionless number that describes how light propagates through that medium. The refractive index determines how much light is

Table 1. Expanded calibration uncertainty for temperature (T) and relative humidity (RH) measurements

Source		Probability distribution		Contribution to uncertainty (°C)
Thermometry bridge resolution		rectangular		1.299E-05
Thermostat bath	homogeneity	rectangular		0.025981
	stability	normal		0.011000
EDIE	stability	rectangular		0.002887
	homogeneity	rectangular		0.113680
Uncertainty of T reference sensor		normal		0.001829
Resolution of T sensor in calibration		rectangular		0.008660
		Sensor T A/IN-C	Sensor T B/IN-B	Sensor T C/OUT
		(°C)		
Repeatability of T sensor in calibration		0.001593	0.001684	0.001990
Interpolation uncertainty U_{int}		0.058283	0.052228	0.060709
Standard uncertainty U_T		0.132	0.130	0.133
Expanded uncertainty U_T (k = 2)		0.264	0.259	0.267
		Probability distribution		Contribution to uncertainty (%)
EDIE	homogeneity	rectangular		0.06062
	stability	rectangular		0.07217
	uncertainty	normal		0.15000
Uncertainty of RH reference sensor		normal		0.31842
Resolution of RH sensor in calibration		rectangular		0.02887
		Sensor RH A/IN-C	Sensor RH B/IN-B	Sensor RH C/OUT
		(%)		
Repeatability of RH sensor in calibration		0.441086	0.638941	0.441086
Interpolation uncertainty U_{int}		1.143929	1.403216	1.471869
Standard uncertainty U_{RH}		1.279	1.585	1.579
Expanded uncertainty U_{RH} (k = 2)		2.559	3.169	3.159

U – expanded uncertainty; U_{int} – interpolation uncertainty

https://doi.org/10.17221/772/2017-PSE

Table 2. Calibration values for solar radiation measurements

	UV-B Sensors			Pyranometer
	IN-C	IN-B	OUT	OUT
Reference value (mW/m^2)	24.8	25.1	23.9	1022 W/m^2
Measured value (mV)	28	28	28	2598 (1039 W/m^2)
Calibration factor (V/(W/m^2))	1.13	1.11	1.17	1.017
K factor (W/m^2 per mV)	0.886	0.896	0.853	0.984
Standard uncertainty U_{SR}	0.299 mW/m^2	0.283 mW/m^2	0.295 mW/m^2	0.025 mV (2.078 W/m^2)
Expanded uncertainty U_{SR} (k = 2)	0.598 mW/m^2	0.567 mW/m^2	0.589 mW/m^2	0.050 mV (4.156 W/m^2)

UV-B SR sensors installed in IN-C, IN-B and OUT and pyranometer installed in OUT. K factor – constant calculated after the calibration test; U – expanded uncertainty

bent or refracted when entering a material, as described by Snell's law (Eq. 3):

$$n = \frac{\sin\theta i}{\sin\theta r} = \frac{v_1}{v_2} = \frac{n_2}{n_1} \quad (3)$$

Where: n – index of refraction; θi – angle of incidence; θr – angle of refraction; v – velocity of light in the medium.

The index of refraction depends on the density of the material, the T and the wavelength of the incident light. If incidence angle is different from zero, increasing angle of incidence increases refraction r.

T and RH are components that can cause a variation on the film's transmissivity (Michel et al. 1986, Priyadarshi et al. 2005). According to Priyadarshi and colleagues, the change of thermo-optic coefficient suggests that the change of refractive index may have a relationship with density. Moreover, according to the Lorentz-Lorenz law (Born and Wolf 1999) (Eq. 4), refractive index is related to density:

$$\frac{n^2-1}{n^2+2} = \frac{\rho RD}{M} \quad (4)$$

Where: ρ – density of material; RD – molar refraction; M – molecular weight. Molar refraction and molecular weight remain nearly constant with changes of T. As the T changes, the refractive index of polymer changes (Eq. 5):

$$\frac{\delta n}{\delta T} = \left(\frac{\delta n}{\delta \rho}\right)_T \left(\frac{\delta \rho}{\delta T}\right) + \left(\frac{\delta n}{\delta T}\right)_\rho = -\left(\frac{\rho \delta n}{\delta \rho}\right)_T \alpha + \left(\frac{\delta n}{\delta T}\right)_\rho \quad (5)$$

Where: δn/δT – temperature-caused index change; α – volume coefficient of a polymer thermal expansion; $(\delta n/\delta T)_\rho$ – index change under constant density; $(\rho\delta n/\delta\rho)_T$ – constant for a given polymer based on the Lorentz-Lorenz law (Zhang et al. 2006).

Statistical analysis. The R package 'Rcmdr' (RStudio Team 2015) was used to perform the statistical analysis by means of: Pearson's correlation coefficient (r); Spearman's rank correlation (ρ); general linear model (GLM) including standard error (SE); residual of SE (RSE); coefficient of determination (R^2). The GLM was used in order to compare the growth, the anthesis, the fruit setting and the LAI values with respect to daily means of RH and T values (calibrated and non-calibrated) and UV-B. A second statistical analysis was performed by comparing the morphological values in combination with UV-B values with respect to RH and T values (calibrated and non-calibrated).

RESULTS AND DISCUSSION

Morphological observations. In the three weeks after transplanting, the tomato plants cultivated in IN-B featured a higher mean growth with respect to the plants cultivated in IN-C (mean difference of about 1 cm). They then had a turnaround on 17 June, with a gap up to 6 cm on 6 July (Figure 1a). A basal leaves damage observed in the last week of June was attributed to a mite infection (*Aculops lycopersici*). A greater damage was noticed (the largest number of affected leaves) in plants grown under diffusive coverage and blocking UV-B (IN-B). Plants grown in OUT showed a lower growth and underwent a lower infectious damage than IN-C and IN-B.

The blooming of the first flower was observed on 17 June in OUT, on 22 June in IN-C and on 24 June in IN-B. In IN-C, anthesis gradually increased for the first three weeks of onset, then slowed down between 1 and 7 July and reached 100% after 6 days. In percentage terms, anthesis in IN-B proceeded slowly compared to IN-C and OUT but with constant increase until 6 July with

https://doi.org/10.17221/772/2017-PSE

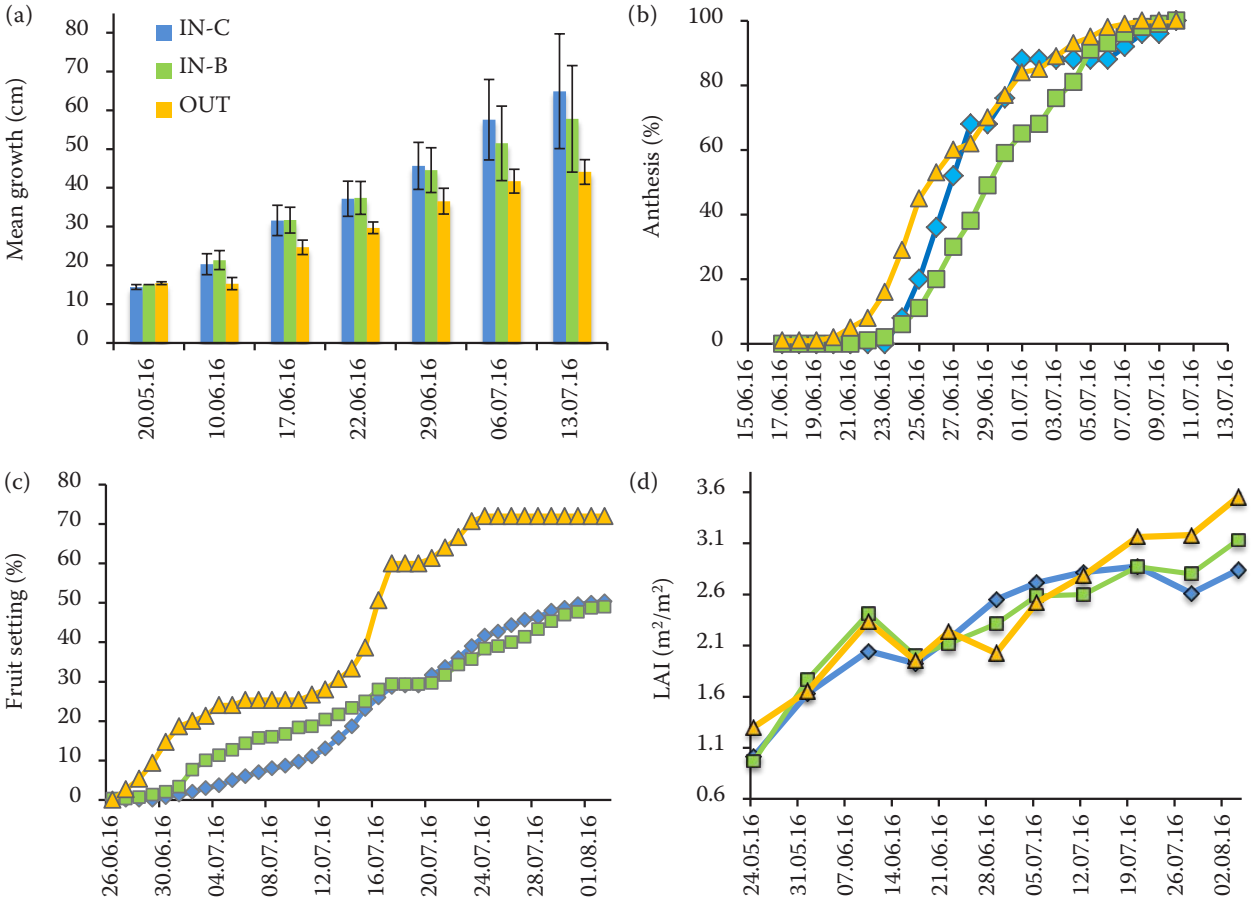

Figure 1. Tomato plants cultivated under transmissive UV-B coverage (IN-C), under diffusive coverage, filtering UV-B (IN-B) and outdoors, without coverage (OUT). LAI – leaf area index

fruit setting around 90%, which then reached 100% in 4 days (Figure 1b).

The fruit setting was observed primary in OUT on 26 June, followed by IN-B on 28 June and IN-C on 2 July. In the first ten days, in percentage terms, in OUT the occurrence of new fruits took place in a gradual and progressive trend, then slowed down around 16 July. The trend of IN-B followed the one in IN-C. However, the trend of IN-C was more uniform but lower than IN-B and OUT. Around 20 July, a reversal trend was observed between IN-C and IN-B (Figure 1c).

Considerations are similar regarding the LAI (Figure 1d). Indeed, in the first three weeks of cultivation a higher mean LAI for plants grown in IN-B compared to those in IN-C was observed, with a maximum difference of 0.37 m^2/m^2 on 10 June. A turnaround on 20 June followed. The reversal of tendency might be due to higher pathogen infection. The mean LAI of plants cultivated in OUT seemed to follow the trend of the plants in IN-B.

Meteorological parameters. Data from all the thermo-hygrometers sensors, calibrated and non-calibrated, were compared. Figures 2a,c show the daily means of T and RH. Differences among the recorded measurements can be appreciated, as well as the dispersion of the T and RH values from the hourly mean in the day (Figures 2b,d for non-calibrated data).

In general, the air T values gathered from data in which the calibration curve were applied were higher than those gathered from the same data without application of the calibration curve, vice versa for RH values.

For all the period studied, the UV-B values recorded in IN-B were 0 W/m^2. In IN-C the values recorded at the beginning of June were in the range from 0 W/m^2 to 4.42 W/m^2, reached the values of 7.08 W/m^2 on 10 July, and with a reversal trend, got 0 W/m^2 after few weeks (Figure 3).

A T comparisons were performed in order to evaluate potential damage of the covering material.

https://doi.org/10.17221/772/2017-PSE

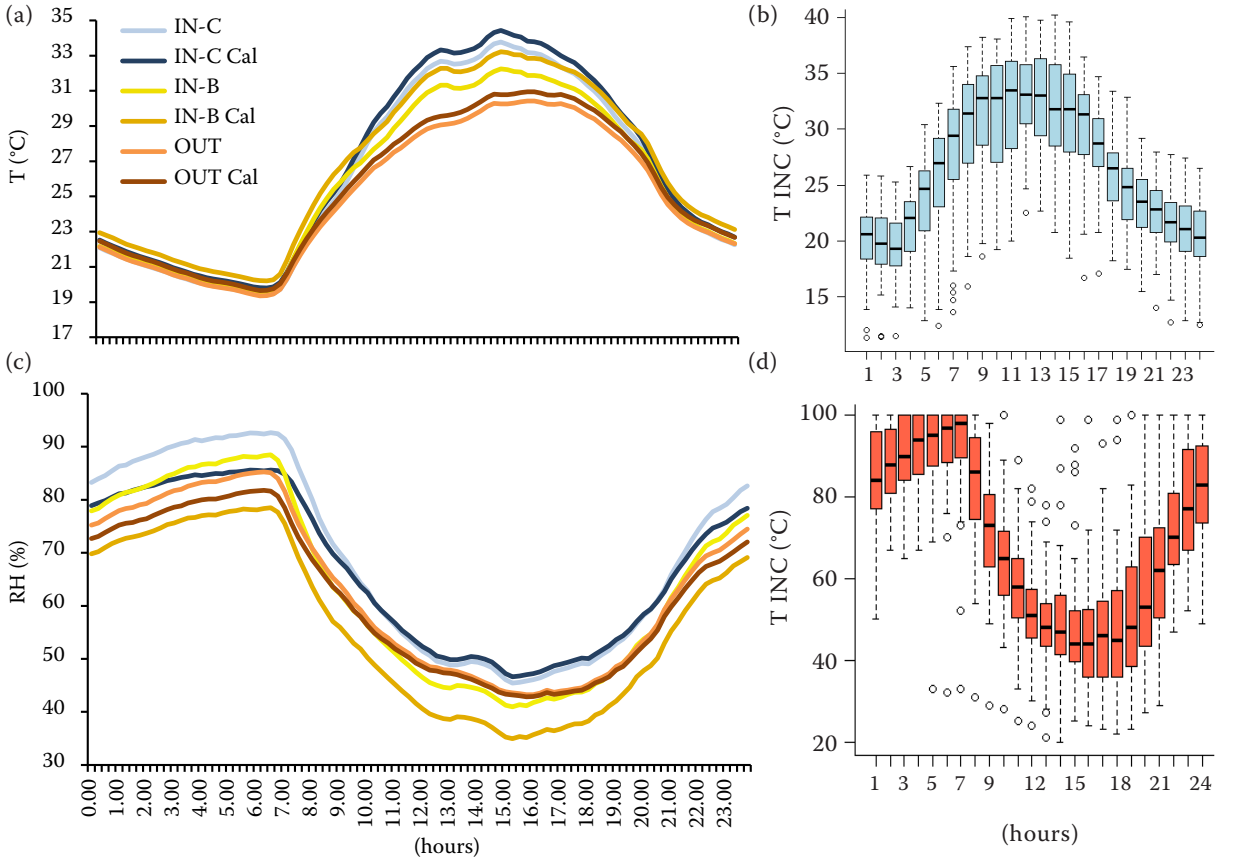

Figure 2. Comparison of daily mean for (a) air temperature (T) and (c) relative humidity (RH) sensors in IN-B, IN-C and OUT, calibrated (Cal) and non-calibrated. Dispersion from the hourly mean of the (b) T and (d) RH values non-calibrated in IN-C in the day

As previously explained (2.4), the thermo-optic coefficient for polymers is T and RH-dependent and, as the T changes, the refractive index of polymeric films changes (Priyadarshi et al. 2005). Further studies are necessary to better evaluate whether the high T recorded, over 40°C, has changed the transmissive feature of the covering material installed in IN-C, also in accordance to Michel (1986), and whether the morphological characteristics of tomatoes have changed their growth, anthesis, LAI and fruit setting trends.

Statistical analysis results. Statistical analyses were carried out regarding the parameters recorded in IN-C, in particular, UV-B measure-

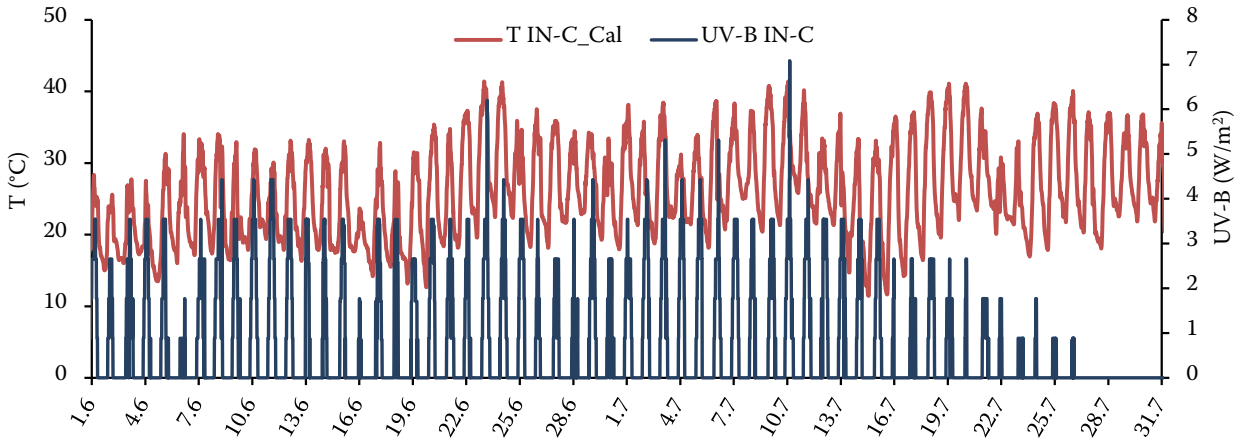

Figure 3. Temperature (calibrated values) and UV-B measurement comparison in IN-C; daily values

https://doi.org/10.17221/772/2017-PSE

Table 3. Pearson's correlation coefficient (r) and Spearman's rank correlation for UV-B measurement in IN-C compared to relative humidity (RH) and temperature (T) values calibrated (Cal) and non-calibrated

	UV-B IN-C ~	Pearson's correlation coefficient		Spearman's rank (ρ)
		P	r	
RH	IN-C Cal	< 2.2e-16	–0.779661	–0.838249
	IN-C	< 2.2e-16	–0.772221	–0.838249
T	IN-C Cal	< 2.2e-16	0.814830	0.843739
	IN-C	< 2.2e-16	0.814794	0.843739

ments compared to RH and T values calibrated and non-calibrated using the Pearson's correlation coefficient (r) and Spearman's rank correlation (ρ) (Table 3). The correlation results were –0.779 and –0.838 for RH, 0.815 and 0.845 for T, respectively, with a P-value < 0.001.

As far the morphological values in IN-C are concern, the GLM was used to compare the growth, the anthesis, the fruit setting and the LAI values in combination with UV-B values with respect to RH and T values (calibrated and not-calibrated). The analysis also included SE, RSE and R^2. As listed in Table 4, all the results were statistically significant (P < 0.001) except for fruits set in combination with UV-B values.

A second statistical analysis was performed comparing the morphological values with respect to RH, T and UV-B values. All GLM results were statistically significant (P in brackets < 0.001). Specifically, R^2 for growth were: 0.8393 (0.00374); 0.8390 (0.00375); 0.9872 (6.26e-06); 0.9872 (6.26e-06) and not assigned (NA) for the comparison with RH measured in IN-C not calibrated, RH in IN-C calibrated; T in IN-C not calibrated; T in IN-C calibrated and UV-B measured in IN-C, respectively. For anthesis R^2 the results were: 0.9898 (< 2.2e-16) for RH in IN-C not calibrated; 0.9895 (< 2.2e-16) for RH in IN-C calibrated; 0.9217 (1.184e-13) for T in IN-C not calibrated and calibrated, NA for UV-B in IN-C. For fruit set, the R^2 results were: 0.1894 (0.0063); 0.1953 (0.0055); 0.1628 (0.0120); 0.1629 (0.0120) and 0.1451 (0.0183) for the comparison with RH in IN-C not calibrated, RH in IN-C calibrated; T in IN-C not calibrated; T in IN-C calibrated and UV-B in IN-C, respectively. As far as the LAI is concerned, R^2 results were: 0.4852 (0.0172) for RH in IN-C not calibrated; 0.4871 (0.0169) for RH in IN-C calibrated; 0.7974 (0.0002) for T in IN-C not calibrated and calibrated and NA for UV-B in IN-C.

The absence of UV-B affected growth and LAI and it influenced the susceptibility of plants to mite infections. The presence of UV-B affected

Table 4. General linear model (GLM) including standard error (SE); residual of SE (RSE) and coefficient of determination (R^2), for morphological parameters and UV-B compared to relative humidity (RH) and temperature (T) values in IN-C

	GLM	SE	RSE	R^2	P
Growth + UVB_INC ~	RH IN-C Cal	11.94	8.166	0.839	0.003753**
	RH IN-C	10.67	8.159	0.8393	0.003739**
	T IN-C Cal	2.867	2.298	0.9872	6.264e-06***
	T IN-C	2.867	2.298	0.9872	6.262e-06***
Anthesis + UVB_INC ~	RH IN-C Cal	NA	4.174	0.9895	< 2.2e-16***
	RH IN-C	NA	4.113	0.9898	< 2.2e-16***
	T IN-C Cal	NA	11.42	0.9217	1.186e-13***
	T IN-C	NA	11.42	0.9217	1.184e-13***
Fruit set + UVB_INC ~	RH IN-C Cal	93.551	51.06	0.2141	0.0400
	RH IN-C	89.729	51.16	0.2110	0.0426
	T IN-C Cal	223.96	51.65	0.1957	0.0573
	T IN-C	228.17	51.65	0.1957	0.0573
LAI + UVB_INC ~	RH IN-C Cal	0.2536	0.4742	0.4871	0.01694*
	RH IN-C	0.2259	0.4751	0.4852	0.01725*
	T IN-C Cal	0.2027	0.298	0.7974	0.00021***
	T IN-C	0.2065	0.298	0.7974	0.00021***

***P = 0.001; **P = 0.01; *P =0.05; NA – not assigned; LAI – leaf area index

https://doi.org/10.17221/772/2017-PSE

T and RH, as confirmed by the T values recorded from calibrated sensors that were higher than those gathered from non-calibrated sensors, vice versa for RH values.

Further studies are necessary to evaluate the measurement uncertainties of meteorological parameters that can affect the crop productivity and the assessment of the quality of products through chemical characterization.

REFERENCES

Bacci L., Grifoni D., Sabatini F., Zipoli G. (1999): UV-B radiation causes early ripening and reduction in size of fruits in two lines of tomato (*Lycopersicon esculentum* Mill.). Global Change Biology, 5: 635–646.

Biswas S.K., Akanda A.R., Rahman M.S., Hossain M.A. (2015): Effect of drip irrigation and mulching on yield, water-use efficiency and economics of tomato. Plant, Soil and Environment, 61: 97–102.

Born M., Wolf E. (1999): Principles of Optics: Electromagnetic Theory of Propagation, Interference and Diffraction of Light. Section 2.3.3. 7th Edition. Cambridge, Cambridge University Press.

Castagna A., Chiavaro E., Dall'asta C., Rinaldi M., Galaverna G., Ranieri A. (2013): Effect of postharvest UV-B irradiation on nutraceutical quality and physical properties of tomato fruits. Food Chemistry, 137: 151–158.

Confalonieri R., Foi M., Casa R., Aquaro S., Tona E., Peterle M., Boldini A., De Carli G., Ferrari A., Finotto G., Guarneri T., Manzoni V., Movedi E., Nisoli E., Paleari L., Radici I., Suardi M., Veronesi D., Acutis M. (2013): Development of an app for estimating leaf area index using a smartphone. Trueness and precision determination and comparison with other indirect methods. Computers and Electronics in Agriculture, 96: 67–74.

Fedina I.S., Velitchkova M.Y. (2009): Physiological responses of higher plants to UV-B radiation 2009. In: Singh S.N. (ed.): Climate Change and Crops. Berlin, Heidelberg, Springer-Verlag.

Fišerová H., Hartman I., Prokeš J. (2015): The effect of weather and the term of malting on malt quality. Plant, Soil and Environment, 61: 393–398.

Hülsen G., Gröbner J. (2007): Characterization and calibration of ultraviolet broadband radiometers measuring erythemally weighted irradiance. Applied Optics, 46: 5877–5886.

Krizek D.T. (2004): Influence of PAR and UV-A in determining plant sensitivity and photomorphogenic responses to UV-B radiation. Photochemistry and Photobiology, 79: 307–315.

Li T., Yang Q.C. (2015): Advantages of diffuse light for horticultural production and perspectives for further research. Frontiers in Plant Science, 6: 704.

Lopardo G., Bellagarda S., Bertiglia F., Merlone A., Roggero G., Jandric N. (2015): A calibration facility for automatic weather stations. Meteorological Applications, 22: 842–846.

Merlone A., Lopardo G., Sanna F., Bell S., Benyon R., Bergerud R.A., Bertiglia F., Bojkovski J., Böse N., Brunet M., Capella A., Coppa G., del Campo D., Dobre M., Drnovsek J., Ebert V., Emardson R., Fernicola V., Flakiewicz K., Gardiner T., Garcia-Izquierdo C., Georgin E., Gilabert A., Grykalowska A., Grudniewicz E., Heinonen M., Holmsten M., Hudoklin D., Johansson J., Kajastie H., Kaykisizli H., Klason P., Knazovická L., Lakka A., Kowal A., Müller H., Musacchio C., Nwaboh J., Pavlasek P., Piccato A., Pitre L., de Podesta M., Rasmussen M.K., Sairanen H., Smorgon D., Sparasci F., Strnad R., Szmyrka-Grzebyk A., Underwood R. (2015): The MeteoMet project – Metrology for meteorology: Challenges and results. Meteorological Applications, 22: 820–829.

Merlone A., Sanna F., Beges G., Bell S., Beltramino G., Bojkovski J., Brunet M., del Campo D., Castrillo A., Chiodo N. (2018): The MeteoMet2 project – Highlights and results. Measurement Science and Technology, 29: 025802.

Michel P., Dugas J., Cariou J.M., Martin L. (1986): Thermal variations of refractive index of PMMA, polystyrene, and poly (4-methyl-1 -pentene). Journal of Macromolecular Science – Part B, 25: 379–394.

Priyadarshi A., Shimin L., Wong E.H., Rajoo R., Mhaisalkar S.G., Kripesh V. (2005): Refractive indices variation with temperature and humidity of optical adhesive. Journal of Electronic Materials, 34: 1378–1384.

RStudio Team (2015): RStudio: Integrated Development for R. Boston, RStudio, Inc.

Sanna F., Cossu Q.A., Roggero G., Bellagarda S., Merlone A. (2014): Evaluation of EPI forecasting model with inclusion of uncertainty in input value and traceable calibration. Italian Journal of Agrometeorology, 3: 33–42.

Sanna F., Calvo A., Deboli R., Merlone A. (2018): Vineyard diseases detection: A case study on the influence of weather instruments' calibration and positioning. Meteorological Applications, 25: 228–235.

Schaepman M.E. (1998): Calibration and characterization of a non-imaging field spectroradiometer supporting imaging spectrometer validation and hyperspectral sensor modelling. [PhD thesis] Zurich, University of Zurich.

Schreiner M., Huyskens-Keil S. (2006): Phytochemicals in fruit and vegetables: Health promotion and postharvest elicitors. Critical Reviews in Plant Sciences, 25: 267–278.

Zhang Z.Y., Zhao P., Lin P., Sun F.G. (2006): Thermo-optic coefficients of polymers for optical waveguide applications. Polymer, 47: 4893–4896.

Received on December 4, 2018
Accepted on April 9, 2018
Published online on May 11, 2018